

Identification of Enterodiol as a Masker for Caffeine Bitterness by Using a Pharmacophore Model Based on Structural Analogues of Homoeriodictyol

Jakob P. Ley,^{*,†} Marco Dessoy,[‡] Susanne Paetz,[†] Maria Blings,[†] Petra Hoffmann-Lücke,[†] Katharina V. Reichelt,[†] Gerhard E. Krammer,[†] Silke Pienkny,[‡] Wolfgang Brandt,[‡] and Ludger Wessjohann[‡]

[†]Symrise AG, Flavor & Nutrition, Research & Technology, P.O. Box 1253, D-37601 Holzminden, Germany

[‡]Leibniz Institute of Plant Biochemistry, Weinberg 3, D-06120 Halle, Germany

S Supporting Information

ABSTRACT: Starting from previous structure–activity relationship studies of taste modifiers based on homoeriodictyol, dihydrochalcones, deoxybenzoins, and *trans*-3-hydroxyflavones as obvious analogues were investigated for their masking effect against caffeine. The most active compounds of the newly investigated taste modifiers were phloretin, the related dihydrochalcones 3-methoxy-2',4,4'-trihydroxydihydrochalcone and 2',4-dihydroxy-3-methoxydihydrochalcone, and the deoxybenzoin 2-(4-hydroxy-3-methoxyphenyl)-1-(4-hydroxyphenyl)ethanone. Starting with the whole set of compounds showing activity >22%, a (Q)SAR pharmacophore model for maskers of caffeine bitterness was calculated to explain the structural requirements. After docking of the pharmacophore into a structural model of the broadly tuned bitter receptor hTAS2R10 and docking of enterolactone and enterodiol as only very weakly related structures, it was possible to predict qualitatively their modulating activity. Enterodiol (25 mg L⁻¹) reduced the bitterness of the 500 mg L⁻¹ caffeine solution by about 30%, whereas enterolactone showed no masking but a slight bitter-enhancing effect.

KEYWORDS: *flavor modifiers, bitter masking, dihydrochalcones, deoxybenzoins, trans-3-hydroxyflavanones, enterodiol*

I INTRODUCTION

Because of the increasing importance of healthier products, sometimes, ingredients are added that can improve the health status of people but show deficits in taste. Another challenge for the taste of food products is the reduction of some common ingredients such as sucrose or other bulk carbohydrates to lower the caloric intake. Unfortunately, in most cases, the flavor of the products is sacrificed; therefore, a huge demand for flavor modifiers showing activity as off-taste maskers¹ or sweet taste enhancers² has developed during the past 10 years. Some potent new bitter masking molecules such as the 1-carboxymethyl-5-hydroxy-2-hydroxymethylpyridinium inner salt,^{2,3} C-glycosides of catechins against bitterness of proanthocyanidins,⁴ some azo-dyes,⁵ and 4-(2,2,3-trimethylcyclopentyl)butanoic acid⁶ against bitterness of sweeteners and some derivatives related to the flavanone homoeriodictyol (HED, **1**, Figure 1)⁷ were developed: hydroxybenzoic acid vanillylamides⁸ and short chain gingerdiones related to hispolone.⁹ During earlier studies, the vanillyl group was identified as a common structural element for a certain masking activity.

The previously published structure–activity concepts^{7,8} starting from HED (**1**), eriodictyol (**2**), and naringenin (**3**) (Figure 1) were extended to evaluate the potential to predict the bitter masking activity of nonobviously related natural products against caffeine by using a pharmacophore model. First of all, some other more obvious structural analogues of the parent flavanones, namely, the related dihydrochalcones (see

Figure 2), and their shorter chain analogues, the deoxybenzoins (Figure 3), and some 3-hydroxyflavanones (dihydroflavonols, Figure 4) were prepared and tested for their masking ability. In a second step, a pharmacophore model was calculated based on structure–activity relationships using the reduction of caffeine bitterness. In a final step, the nonobvious mammalian lignan metabolites enterodiol and enterolactone were tested in the pharmacophore model as well as in sensory tests for their caffeine bitterness modulating activity.

M MATERIALS AND METHODS

Phloretin, naringenin-7-*O*-glucosid, and phloridzin [each >95%, high-performance liquid chromatography (HPLC)] were from Kaden Biochemicals (Hamburg), ampelopsin was from Changsha Sunfull Biotech Co., Ltd. (China), 2-(3,4-dihydroxyphenyl)-1-(2,4-dihydroxyphenyl)-ethanon was from Toronto Chemicals (Ontario, Canada), and enterodiol and enterolactone were from Phytolab (Verstenbergsgreuth, Germany). All other test compounds were synthesized according to principally known procedures as outlined in the Supporting Information.

Syntheses. 2-(4-Hydroxy-3-methoxyphenyl)-1-(4-hydroxyphenyl)ethanone (**18**). Guajacol (2-methoxyphenol, catechol monomethylether, 2.0 g, 16.1 mmol) and 4-hydroxyphenylacetic acid (2.4 g, 16.1 mmol) were cooled to 0 °C, and 35 mL (322 mmol) boron trifluoride etherate was added. The mixture was slowly heated

Received: March 28, 2012

Revised: June 4, 2012

Accepted: June 7, 2012

Published: June 7, 2012

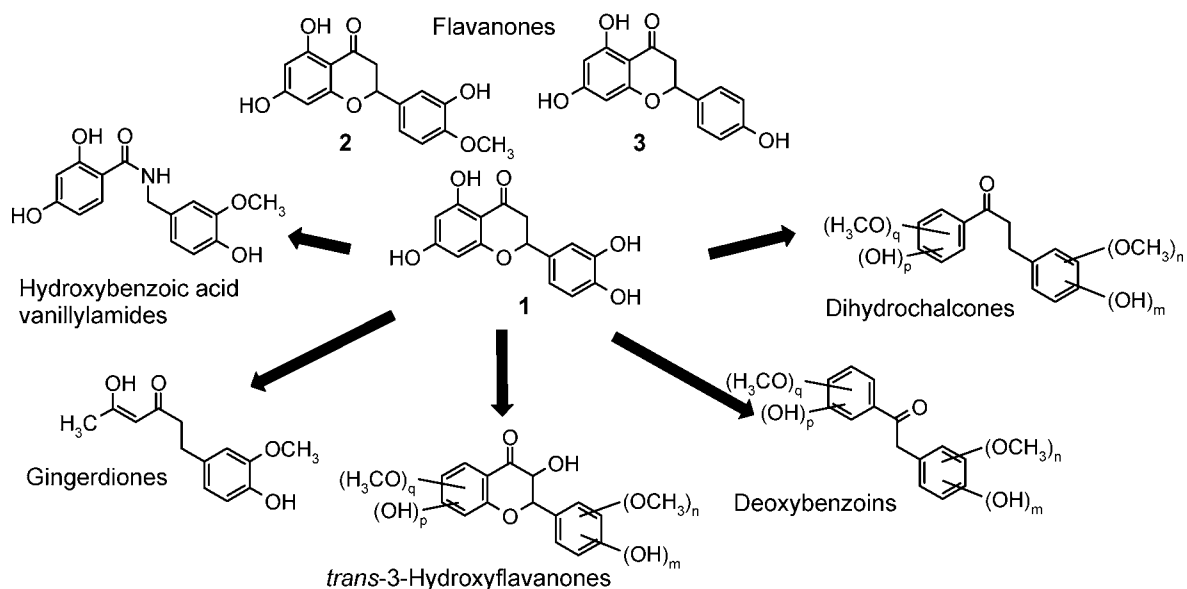


Figure 1. Investigated structural classes related to HED (1), eriodictyol (2), and naringenin (3).

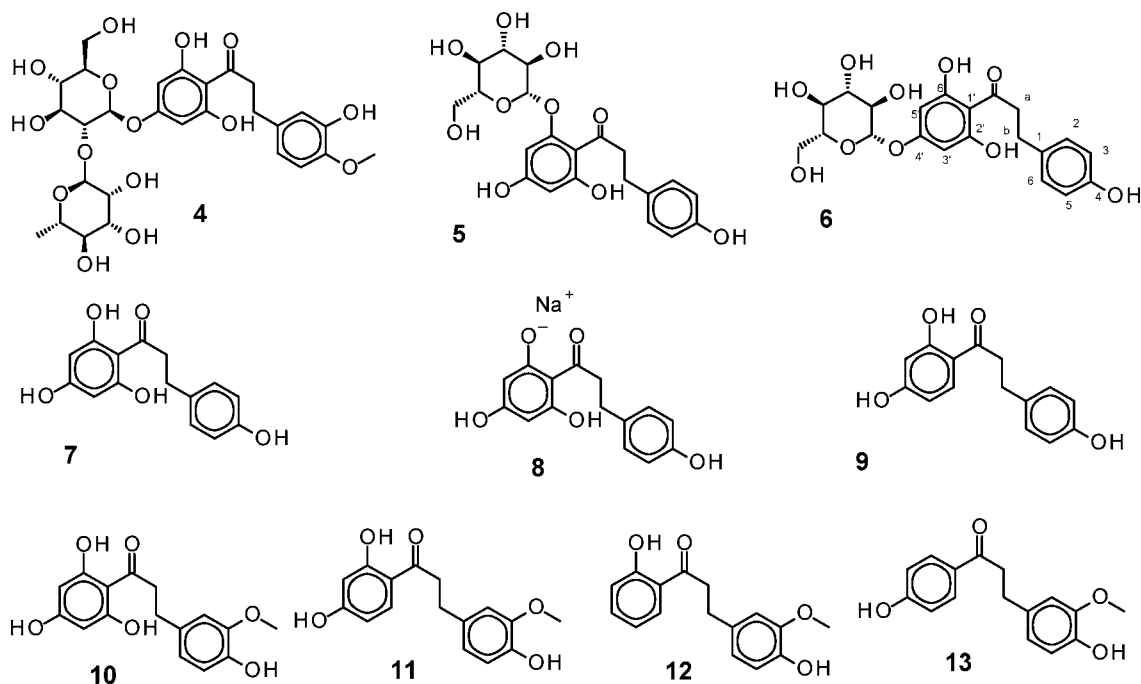


Figure 2. Investigated dihydrochalcones 4–13 [NHDC (4), phloridzin (5), trilobatin (6), phloretin (7), and davidigenin (8)].

to 90 °C for 13 h (TLC control $\text{CHCl}_3/\text{MeOH}$ 10:1, $R_f = 0.4$). BF_3 -etherate was distilled, and the cooled residue was quenched with water/ethyl acetate (100 mL, 1:1) under vigorous stirring. The organic phase was separated, and the water phase was extracted again with 50 mL of ethyl acetate. The combined organic phases were washed with NaHCO_3 solution and brine, and dried over Na_2SO_4 concentrated, keeping the product in solution. After treatment with ethyl ether, the white product precipitated as a white solid (purity by ^1H NMR, 97%), which was recrystallized from ethyl acetate. Yield, 59 mg (14%). HPLC-MS (RP-18, APCI⁻): $m/z = 257.38$ (100%, $[\text{M} - \text{H}]^-$). HRMS (ESI⁻, $\text{M} - \text{H}$) calcd for $\text{C}_{15}\text{H}_{13}\text{O}_4$, 257.0819; found, 257.0818; (ESI⁻, $\text{M} - \text{H}$) calcd for $\text{C}_{15}\text{H}_{15}\text{O}_4$, 259.0965; found, 259.0976. ^1H NMR (400 MHz, $\text{DMSO}-d_6$, internal standard TMS): $\delta = 9.97$ (1H, bs, OH), 9.24 (1H, bs, OH), 7.60 (1H, dd, $J = 8.3$ Hz, $J = 2.0$ Hz, H-2), 7.48 (1H, d, $J = 2.0$ Hz, H-6), 7.05 (2H, m, H-2', H-6'), 6.85 (1H, d, $J = 8.3$ Hz, H-3), 6.68 (2H, m, H-3', H-5'), 4.12 (2H, s, H-a) ppm. ^{13}C

NMR (100 MHz; $\text{DMSO}-d_6$, internal standard TMS): $\delta = 196.1$ (C, C- α), 155.8 (C, C-4'), 151.6 (C, C-4), 147.4 (C, C-3), 130.2 ($2 \times \text{CH}$, C-2', C-6'), 128.0 (C, C-1), 125.6 (C, C-1'), 123.5 (CH, C-6), 115.0 ($2 \times \text{CH}$, C-3', C-5'), 114.8 (CH, C-5), 111.5 (CH, C-2), 55.5 (CH_3 , O- CH_3), 43.3 (CH_2 , C- β) ppm.

2-(4-Hydroxyphenyl)-1-(2,4,6-trihydroxyphenyl)ethanone (20). 4-Hydroxybenzylcyanide (2.60 g, 20 mmol) and 1,3,5-trihydroxybenzyl (3.78 g, 30 mmol) were mixed with 1,4-dioxan (30 mL) and treated with dry HCl for 5 h. The mixture was stirred at room temperature for another 16 h. The precipitate was filtered off, and the raw crystalline material (6.34 g) was diluted with ice water (15 mL) and refluxed for 1 h. After it was cooled, the precipitate was filtered off, washed with water, and dried in vacuo. Yield, 3.0 g (colorless crystals, 11.5 mmol, 58% of theory). HPLC-MS (RP-18, APCI⁻): $m/z = 259.44$ (100%, $[\text{M} - \text{H}]^-$), 518.88 (14%, $[2\text{M} - \text{H}]^-$). HRMS (ESI⁻, $\text{M} - \text{H}$) calcd for $\text{C}_{14}\text{H}_{11}\text{O}_5$, 259.0612; found, 259.0623; (ESI⁺, $\text{M} + \text{H}$) calcd for

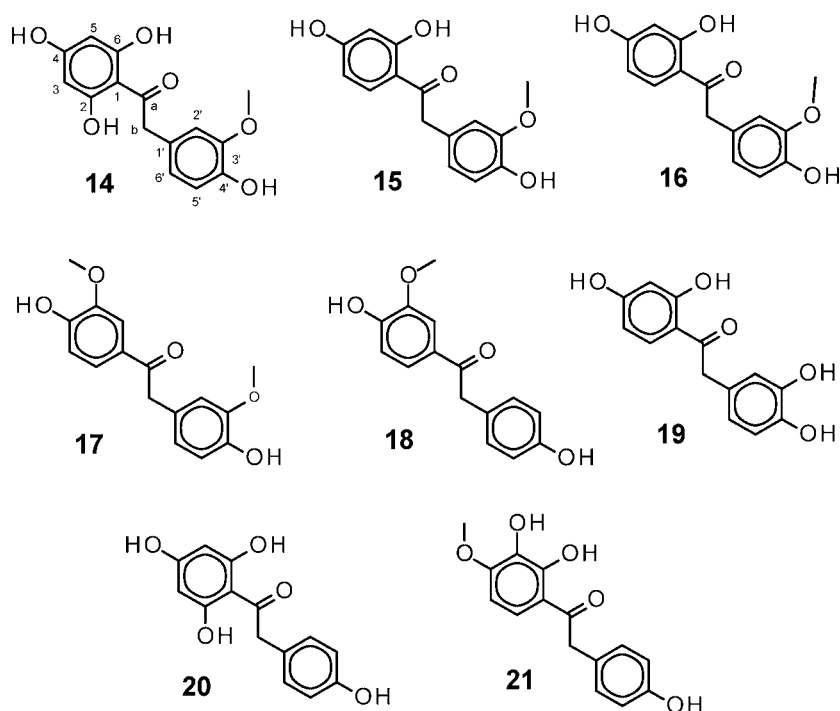


Figure 3. Investigated deoxybenzoins 14–21.

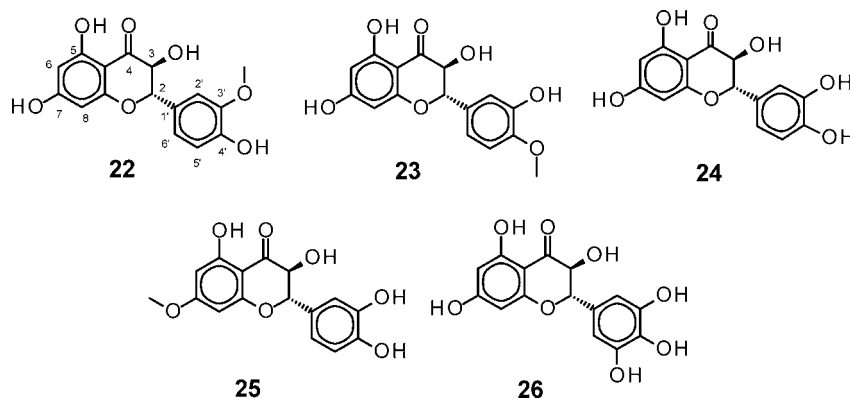


Figure 4. Structures of *trans*-3-*O*-hydroxyflavanones 22–26 [blumeatin A (23) and ampelopsin (26)].

$C_{14}H_{13}O_5$, 261.0757; found, 261.0762. 1H NMR (400 MHz, $DMSO-d_6$, internal standard TMS): δ = 12.23 (ca. 2H, s, OH), 10.37 (1H, s, OH), 9.19 (1H, s, OH), 7.01 (2H, m, H-2', H-6'), 6.67 (2H, m, H-3', H-5'), 5.81 (2H, s, H-3, H-5), 4.21 (2H, s, H- α) ppm. ^{13}C NMR (100 MHz; $DMSO-d_6$, internal standard TMS): δ = 202.9 (C, C=O), 164.7 (C, C-4), 164.1 (2 \times C, C-2, C-6), 155.7 (C, C-4'), 130.4 (2 \times CH, C-2', C-6'), 125.8 (C, C-1'), 114.8 (2 \times CH, C-3', C-5'), 103.5 (C, C-1), 94.6 (2 \times CH, C-3, C-5), 47.9 (CH_2 , C- α) ppm.

Sensory Studies. Bitter taste modulating studies were done using a duo-comparison method with a panel of trained healthy adults (7 males and 15 females; ages 25–48 years) without any reported taste disorder. Tasting sessions were carried out in the morning hours 1–2 h after breakfast, during which time the panelists were asked not to drink black or green tea or coffee due to adaptation to caffeine. Duo tests were presented to the testers in a randomized order; in case of discoloration, samples were covered with aluminum foil or tasted under colored light. Panel members were trained to evaluate the taste of aqueous solutions (5 mL each) of the following standard taste compounds: citric acid (0.4 g L^{-1}) for sour taste, caffeine (0.3 g L^{-1}) for bitter taste, sodium chloride (1.3 g L^{-1}) for salty taste, sucrose (6.0 g L^{-1}) for sweet taste, and monosodium glutamate (0.4 g L^{-1}) for umami taste. Difference tests were carried out for the basic tastes: citric acid (0.5 and 0.6 g L^{-1}), caffeine (0.25 and 0.35 g L^{-1}), sodium

chloride (1.5 and 1.8 g L^{-1}), sucrose (8.0 and 10.0 g L^{-1}), and monosodium glutamate (3.6 and 4.4 g L^{-1}) using paired comparison test.

For bitter modulating tests, the panelists had to rate the intensity (*I*) of the bitterness on a scale of 1 (nothing) to 10 (extremely strong). The mean rating of 500 kg L^{-1} caffeine solution ranged between 5 and 6. For other bitter tastants (quinine, KCl, and salicin), concentrations were used at which all panelists can perceive a pronounced bitterness (mean ratings about 4–6). Modulation effects (MEs, as %) were calculated relative to the blind probe using the equation:

$$ME = (I_{\text{test}} - I_{\text{blind}}) / I_{\text{blind}}$$

Negative ME values were interpreted as inhibitory, and positive values were interpreted as enhancing effects. Statistical analysis was performed using internal functions of MS Excel 97 (Microsoft Corp.). Student's *t* test (double-sided, paired) was used to calculate statistical significance.

Molecular Modeling. All 3D structures of the compounds were constructed with MOE¹⁰ and were subsequently minimized with the Merck MMFF94 force field.^{11–15} Twenty-one compounds with a bitter masking activity higher than 22% (see Table 1) were considered as active and used for three-dimensional superposition. For this

Table 1. Evaluation of MEs for Bitter Taste of Dihydrochalcones as Compared to HED (1), Eriodictyol (2), and Naringenin (3) against 500 mg L⁻¹ Caffeine^a

compd	bitter modulation 500 mg L ⁻¹ caffeine		profile (100 mg L ⁻¹ in 5% sucrose)
	panelists all/masking	ME for bitter taste	
1 ^b	10/10	-43%*	weak, sweet, vanillic, phenolic
2	16/12	-46%**	neutral
3	9/5	-9%	dry-dusty, fatty, creamy
4	16/8 (3 mg L ⁻¹)	-8%	neutral, long lasting sweetness
	16/6 (30 mg L ⁻¹)	+7%	
5	16/4	+10%	bitter
6	16/2 (50 mg L ⁻¹)	+21%	vanillin, honey, fruity, weak
7	16/3 (50 mg L ⁻¹)	-29%*	sweet, mouth feel, dusty
8	16/9	-6%	balsamic, weak, bitter, licorice
9	15/7	0%	weak, fruity, bitter
10	16/8	-9%	weak, smooth, balsamic, smoky
11	15/11 (50 mg L ⁻¹)	-24%	neutral
12	16/9	-7%	weak, fruity, herbal, dusty
13	15/12 (50 mg L ⁻¹)	-27%*	neutral

^aTest concentration, 100 mg L⁻¹; *, significant ($p < 0.05$); **, $p < 0.005$; ND, not determined. ^bRef 7.

purpose, the “pharmacophore elucidator” module of MOE was used. In this process, all single bonds were allowed to be rotatable, and pharmacophores like hydrogen bond donor and acceptor sites as well as hydrophobic areas were applied in the unified scheme of MOE. On the basis of these calculations and superposition of all active structures, a pharmacophore model was derived manually.

A homology model of the human hTas2R10 based on the X-ray structure 1U10¹⁶ (bovine rhodopsin) has been taken from the model database MODBASE¹⁷ (Q9NYW0, model original ID: EN ENSP0000240619). Because analysis with PROCHECK¹⁸ and PROSA II¹⁹ indicated a not perfectly folded 3D structure, the protein model has been improved by a molecular dynamics simulation (50 ns, including a membrane composed of PEA in a water box) with YASARA^{20,21} using the force field AMBER03²² and the md-runmembrane protocol of YASARA. Here, the conformation of extracellular loop 2 has changed most in comparison to the original MODBASE model. Overall, the quality of the model has improved according to the evaluation with PROCHECK (amino acids in most favored region from 85.2 to 85.5%, two outliers) and the z score of the pair potential of C α and C β of PROSA II (from 0.53 to -1.83).

The ligands enterodiol and enterolactone have been docked into the active site of the hTas2R10 model using GOLD²³ with the N ϵ of Trp 88 as the center of a sphere with a radius of 12 Å. The used Fitness Function was GoldScore.

RESULTS AND DISCUSSION

Syntheses. Most of the investigated compounds were not commercially available and were therefore synthesized by principally known procedures. With the exception of bitter-sweet phloretin glycosides from apple (*Malus* spp.), dihydrochalcones were only rarely found in nature, for example, davidigenin (9) as a trace in *Artemisia dracunculus*.²⁴ The naturally occurring trilobatin (6) (e.g., isolated from *Malus trilobata*, *Vitis* spp., and *Symplococcus* spp.²⁵) was isolated as a side product from a mild acidic hydrolysis of naringin dihydrochalcone. The spectral data of the product correspond to the published data from literature. Phloretin sodium salt was prepared by exchange of protons by using 1 equiv of sodium

ethylate solution and subsequent evaporation of the solvents. The dihydrochalcones 9–13 were synthesized starting with Knoevenagel condensation of the acetophenons with the appropriate benzaldehydes and subsequent hydrogenolysis of the intermediate chalcones. Deoxybenzoins are still much more rarely reported as natural compounds, for example, deoxyvanilloin (14) as a trace compound in the root wood of *Melicope semecarpifolia*.²⁶ The commercially unavailable deoxybenzoins 15–21 were synthesized according to the well-known BF₃·Et₂O-catalyzed Friedel–Crafts acylation of phenols with the appropriate phenylacetic acids.^{27,28} In the case of the tetrahydroxylated deoxybenzoins 14, the alternative route via the corresponding phenyl acetonitrile facilitated by the use of dry HCl was much more successful.²⁹ The deoxybenzoins 18 and 21 were never described in the literature. The investigated *trans*-3-hydroxyflavanones are all known from the literature. Taxifolin (24) is a well-known natural compound, and blumeatin A (23) was described in *Blumea balsamifera*.³⁰ The vanilloid isomer 22 occurs as trace component (5 mg/kg) besides HED (1) in *Lychnophora granmongolense* (“Brazil arnica”),³¹ whereas the isomer 25, which is related to the flavanone sterubin, was also found in *Blumea balsamifera*.³² Dihydromyricetin or ampelopsin (26) was found in *Ampelopsis cantoniensis*.³³ The synthesis of the racemic compounds was performed starting with perbenzylation of the parent flavanones HED (1), hesperetin, or sterubin, subsequent epoxidation in alkaline medium using hydrogen peroxide, and finally hydrogenation to the corresponding *trans*-3-hydroxyflavanones 22, 23, and 25.

Sensory Studies. All compounds were first tested in 5% sucrose and 0.5% sodium chloride solution for the general taste profile (for screening data, see Tables 1–3). Only in the

Table 2. Evaluation of MEs for Bitter Taste of Deoxybenzoins against 500 mg L⁻¹ Caffeine^a

compd	bitter modulation 500 mg L ⁻¹ caffeine		profile (100 mg L ⁻¹ in 5% sucrose)
	panelists all/masking	ME for bitter taste	
14	16/10	-23%	vanillin, spicy, clove, woody, balsamic
15	15/7	-10%	neutral
16	14/8	-9%	sweet, dry-dusty, balsamic
17	14/10	-15%	neutral
18	15/12 (50 mg L ⁻¹)	-29%* ($p < 0.06$)	vanillin, phenolic, balsamic, somewhat bitter
19	15/9	-18%	vanillin, balsamic, woody
20	ND		very bitter, astringent
21	16/10 (50 mg L ⁻¹)	-8%	vanillin, phenolic, sweet

^aTest concentration, 100 mg L⁻¹; *, significant ($p < 0.05$); ND, not determined.

absence of strong off-tastes, the compounds were tested for their bitter modulation activity. Caffeine was selected as a screening vehicle for bitter masking effects due to its activation spectrum of various bitter receptors including the broadly tuned hTAS2R10,³⁴ acceptable taste, and low toxicity. From previous studies, it is known that HED (1) and its structural relatives depicted in Figure 1 show a comparable pattern of activity against various bitter compounds, for example, quinine, which is similar to caffeine, can activate several human bitter receptors including hTAS2R10.³⁴ Until now, the mechanism

Table 3. Evaluation of MEs for Bitter Taste of *trans*-3-Hydroxyflavanones against 500 mg L⁻¹ Caffeine^a

compd	bitter modulation 500 mg L ⁻¹ caffeine		profile (100 mg L ⁻¹ in 5% sucrose)
	panelists all/masking	ME for bitter taste	
22	15/6	+15%	fatty, oily
23	16/9 (50 mg L ⁻¹)	-14%	guaiacol, vanillin, sweet
24	14/4	+18%	very bitter
25	ND		herbal, bitter, phenolic, woody, balsamic
26	14/4	+16%	dry dusty, grape, grape seed

^aTest concentration, 100 mg L⁻¹; *, significant ($p < 0.05$); ND, not determined.

behind the activity of **1** and its analogues has not been known, but they seem to block at least one of these bitter receptors, which are activated by a larger set of bitter molecules.

The best bitter taste reducers for caffeine were the dihydrochalcones phloretin (**7**), **11**, and **13** and the deoxybenzoin **18**. Whereas **11**, **13**, and **18** show the vanilloyl moiety similar to **1**, the activity of phloretin is somewhat surprising. In earlier studies, the simple *para*-hydroxy-substituted derivatives [e.g., naringenin (**3**), 2,4-dihydrobenzoic acid 4-hydroxybenzylamide, [2]-gingerdione, Figure 1] did not show any significant masking activity.^{7,9,29} The short-chain analogue **20** is only moderately active as a flavor modifier, and the glucoside phloridzin (**5**) induces some additional bitterness. Unfortunately, from all tested *trans*-3-hydroxyflavanones, only **23** showed a moderate bitter masking activity toward caffeine. The other analogues exhibit bitter or even bitter-enhancing effects in contrast to their corresponding flavanones. Interestingly, NHDC (**4**) showed no masking activity up to 30 mg L⁻¹ against caffeine bitterness. The use of NHDC as a bitter masker

for pharmaceutical actives has been known for a long time,³⁵ but the strong sweet taste at higher concentrations often cannot be tolerated in all applications.

The most promising bitter taste modulators **7**, **11**, **13**, and **18** for caffeine were tested in more detail. First of all, dose-response plots were determined for caffeine with different concentrations of the test compounds (Figure 5). All four components showed an increasing dose response up to 50 mg L⁻¹, but then, the activity decreased somewhat at 100 mg L⁻¹; probably, the masking activity is competed by arising intrinsic bitterness at higher concentrations (as found, for example, for compound **18** at 100 mg L⁻¹), which may compete with their masking effect. Because of the number of 25 different hTas2R bitter receptors in human,^{34,36} this might be an overlapping effect of antagonistic and agonistic activity as described for certain sesquiterpene lactones³⁷ for different receptor types, which should be investigated in the future.

A subset of the antagonistic pattern of the modulators was investigated as shown in Figure 6; modulating activities lower than 10% are not considered for the discussion. Again, phloretin (**7**) and the dihydrochalcone **11** showed a non-significant activity against quinine, whereas the remaining candidates were not active at the tested concentrations. Only **7** was weakly active as a masker for salicin, whereas the activity of all compounds against KCl or peptides was not detectable. As a summary, phloretin (**7**) seems to be a relatively broadly active bitter taste reducer comparable to HED (**1**), whereas the other compounds found in the screening seem to be active only against caffeine. However, in contrast to **1**, phloretin seems to be limited at a higher dosage due to its own bitter taste at these concentrations.

Structure–Activity Relationships. The concept of structural variation of the parent HED (**1**) seems to work in principle but is not valid for all cases. Therefore, the vanilloyl moiety is probably not solely responsible for the bitter masking

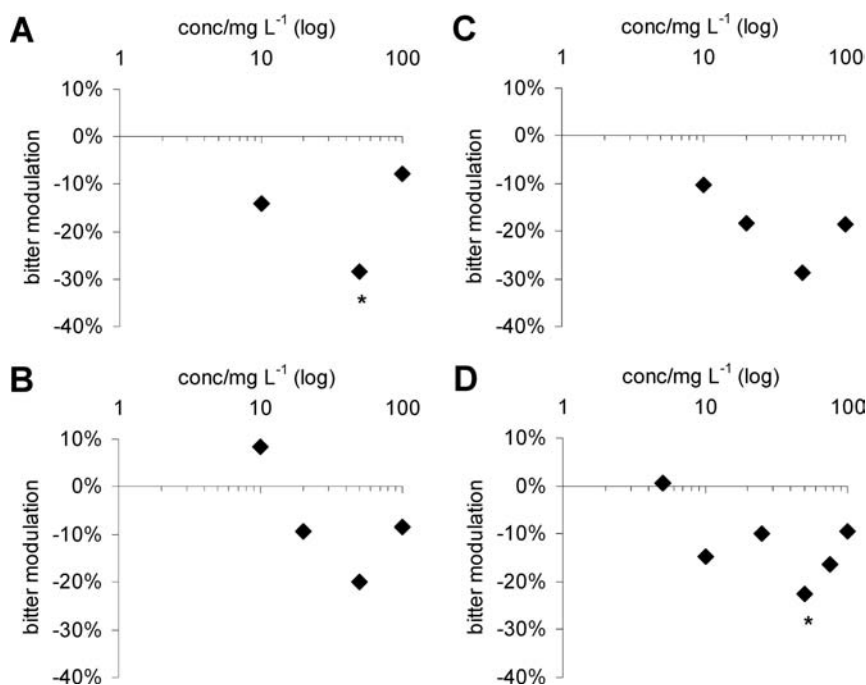


Figure 5. Dose–response plots of masking activities of phloretin (**7**) (A), dihydrochalcones **11** (B), **13** (C), and deoxybenzoin **18** (D) in 500 mg L⁻¹ caffeine solution ($n = 15–16$). *, significant ($p < 0.05$).

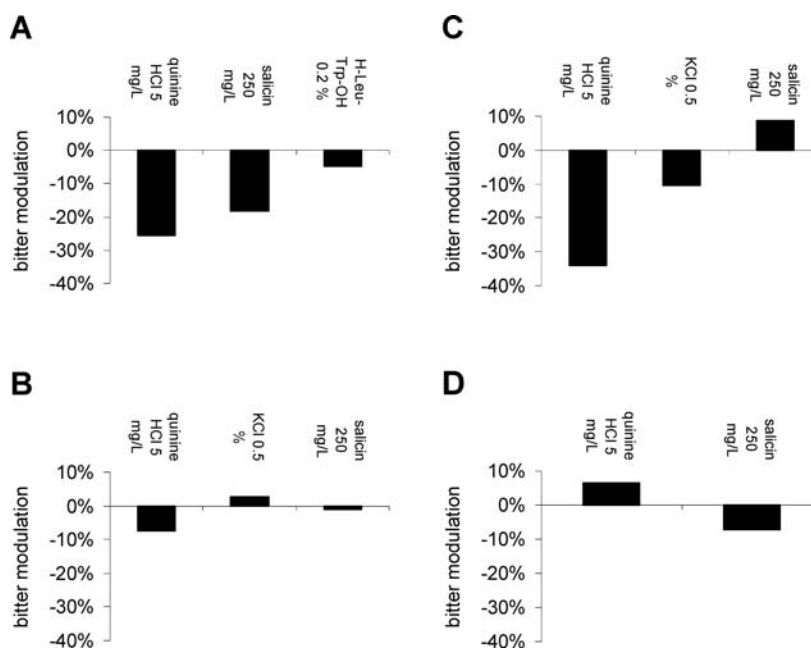


Figure 6. Masking activity of phloretin (**7**) (A, 30 mg L⁻¹), dihydrochalcones **11** (B, 50 mg L⁻¹), **13** (C, 50 mg L⁻¹), and deoxybenzoin **18** (D, 50 mg L⁻¹) for various bitter compounds (relative expressions).

effects of **1**. To study the SAR in a more general sense, a first simplified computational study based on the active (and inactive) compounds was done, whereby 22% bitter masking, that is, ca. half of the HED activity value, was set as a lower threshold for compounds defined as active.

The best result for the superposition of the structures is displayed in Figure 7 together with the pharmacophore

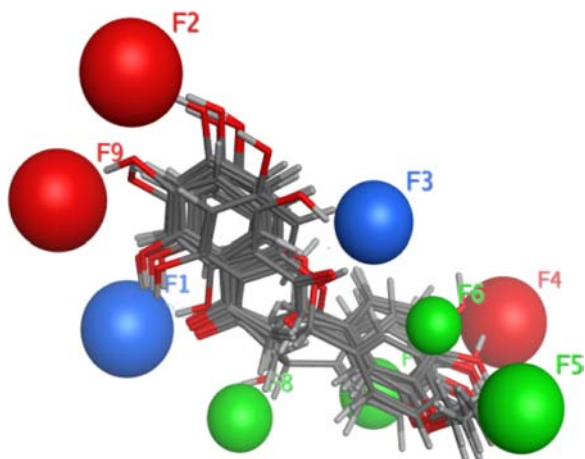


Figure 7. Superposition of all 21 active compounds and derived pharmacophores F1–F9. Red spheres (features F2, F4, and F9) represent proton acceptor sites, blue ones (F1 and F3) represent either proton acceptor and/or donor sites, and the green spheres (F5, F6, and F8) represent preferred hydrophobic interaction areas.

(“gustophore”) model, a simplified counterpart of the mutualized overlay of reasonable conformations of the structures of active compounds. Herein, red spheres (the features F2, F4, and F9) represent proton acceptor sites, blue ones (F1 and F3) either proton acceptor and/or donor sites, and the green ones (F5, F6, and F8) preferred hydrophobic interaction areas.

Eriodictyol (**2**) shows the highest activity with a bitter masking rate of 46% (see Table 1). On the basis of the pharmacophore model, this high activity can be perfectly explained by the model (Figure 8A). Except for the hydrophobic binding site F5, all other areas defined by the suggested pharmacophore are accessible by a low energy conformation of the compound. Both hydroxyl groups of ring B can interact with the proton acceptor feature F4, with the meta-hydroxyl group being preferred for such an interaction. For comparison, in HED (**1**), the methyl group of the 3'-methoxyl moiety of ring B can interact with the hydrophobic area F5 by rotating the phenyl group by 180°. This explains the similar activities but also the differences of **1** and **2**. The removal of the 3'-hydroxyl group in ring B (naringenin, **3**) will lead to an almost complete loss of interaction with both the proton acceptor site F4 and the hydrophobic site F5, resulting in a considerably reduced activity (9%).

Among the compounds **4**–**13** (Table 1), only compounds **7** (29%), **11** (24%), and **13** (27%) exhibit significant bitter masking activity. Because of the conformational flexibility of these compounds, the ring B is able to adopt a conformation in which the *para*-hydroxyl group can service the proton acceptor site F4 (Figure 8B). Additionally, and in difference to compounds **1**–**3**, the additional hydroxyl group at ring A in compound **7** is able to interact with the proton acceptor/donor site F3 quite nicely. Except for the hydrophobic binding site F5, all pharmacophores are satisfied, which may explain the rather high activity of **7** but also of **11** where F5 is occupied instead F3 (Figure 8C).

The inactivity of compounds **4**–**6** can be simply explained by steric overlap especially with binding sites at pharmacophores F2, F9, or/and F1. The lower activity of compound **10** in comparison to **11** might be explainable by slightly different conformational behavior caused by the additional hydroxyl group in ring A. Whereas the ethylene moiety in **11** is highly flexible, a steric hindrance with both *ortho*-hydroxyl groups of ring A in **10** leads to a more perpendicular orientation of the

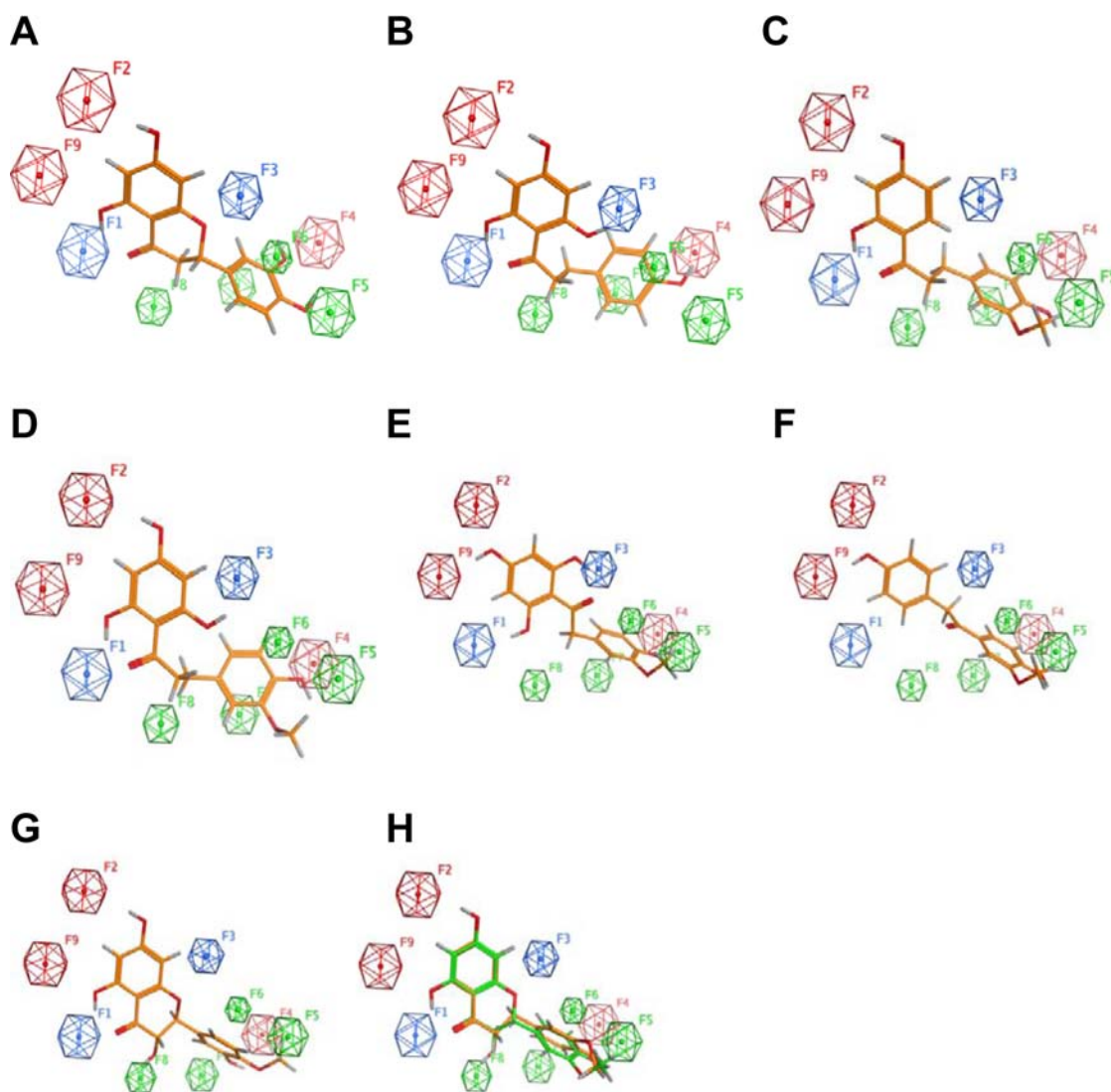


Figure 8. Minimized conformation and interaction of pharmacophore model and (A) eriodictyol (**2**), (B) phloretin (**7**), (C) dihydrochalcone (**11**), (D) compound **10**, (E) deoxybenzoin (**14**), and (F) deoxybenzoin (**18**). The orientation within the model is inverted with respect to the A and B ring position as compared to the best fit of derivative **14**. (G) Blumeatin A (**23**) and (H) comparison of the conformations of HED **1** (green) and 3-hydroxyflavanone **22** (orange carbon atoms).

ethylene group with respect to ring A, which causes difficulties for ring B to interact especially with pharmacophore F5 (Figure 8D).

The deoxybenzoin very likely exhibit a slightly different binding mode in the pharmacophore in comparison to the flavonoids. Because of the reduced conformational flexibility (methylene bridge instead ethylene), their ring B can only interact with F4 or F5 of the pharmacophore, if the carbonyl group simultaneously interacts with F3 but not with F1. Only in this way, the activity of **14** (23%, Table 2 and Figure 8E) can be explained based on the pharmacophore model. Compounds **15** and **16** lack this hydroxyl, which might be a reason for their reduced activities (10 and 9%, respectively). In compound **21** (8%), the *para*-methoxyl group of ring A leads to missing or repulsive interaction with the proton acceptor site F9, whereas this site is occupied in compound **19** (18%), leading to higher activity.

Since in **18** a 3-methyl group is introduced in ring A but no hydrophobic feature exists close to F2 and F9 (Figure 8F), an optimal superposition with the pharmacophore is only possible,

when the compound is posed in an opposite orientation, that is, ring A and ring B exchange their position within the pharmacophore as compared to all previously discussed compounds. Then, the hydroxyl and methoxyl groups of ring A interact with features F4 and F5, and the hydroxyl group of ring B interacts with either F2 or F9. This hypothesis is supported by the introduction of an additional methoxyl group in compound **17**, which leads to reduced affinity in comparison to compound **18** because of the missing hydrophobic feature close to F2 and/or F9.

The *trans*-3-hydroxyflavanones (Table 3) adopt a slightly different conformation in comparison to the flavanones of Table 1 since the 3-hydroxy group causes some repulsion with ring B (Figure 8H). In compound **22** (−15%), the 3-hydroxyl group will cause repulsive interactions with the hydrophobic pharmacophore F8. An interaction of the *meta*-methoxyl group of ring B with the hydrophobic site F5 is also reduced, which obviously contributes to the inactivity of this compound. This holds true also for the inactive compounds **24** and **26**. The special importance of site F5 is supported by the recovered

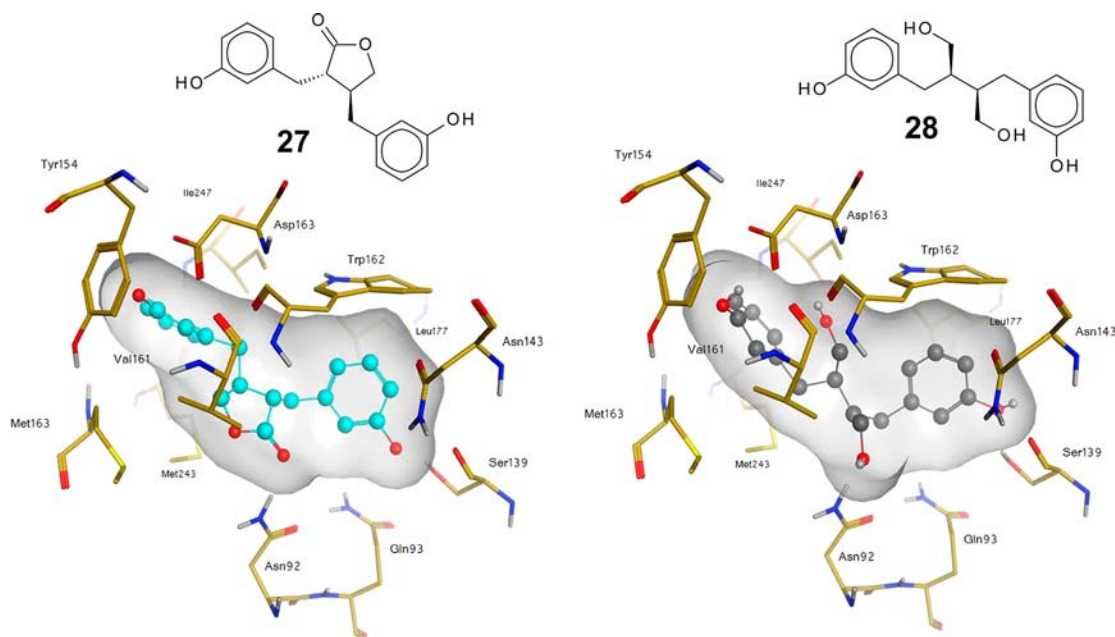


Figure 9. Poses of enterolactone (**27**, carbon atoms in cyan) and enterodiol (**28**, carbon atoms in gray) docked in the active site of the hTas2R10 protein model (carbon atoms in yellow) and additional interaction of enterodiol's hydroxyl group with the carbonyl group of Trp 162, which is missing in enterolactone.

activity of compound **23** (14%) in which the *para*-methoxyl group is now able to interact with this pharmacophore feature (Figure 8G).

Pharmacophore Docking and Prediction of Activity.

In a second step, the mammalian lignans enterolactone (**27**) and enterodiol (**28**, Figure 9) were chosen as related but not obvious test vehicles for prediction of bitter masking activity.

A protein model of one of the broadly tuned bitter receptors, hTas2R10, based on the X-ray structure of bovine rhodopsin in its inactive conformation has been developed. Docking of the structures of **27** and **28** into the active site of hTas2R10 led to similar poses for both but for enterodiol (**28**) without significant distortions of the protein.

The structures used for the pharmacophore (Figure 7) have been aligned with the docking poses of both lignans. Now, the pharmacophore features compare favorably to certain amino acid side chains of the bitter receptor model. The proton acceptor features F2 and F9 localize with the side chain of Asn 173 and the backbone of Ser 139. The proton acceptor and donor features F1 and F3 are in the places of either the side chains of Gln 93 and Asn 92 or the backbone of Trp 162. The proton acceptor feature F4 is located near the side chain of Asp 163. Hydrophobic interaction areas as represented by F5–8 find a counterpart in the protein model with the amino acids Met 243, Ile 247, Leu 259, and Met 263.

The suggested pharmacophore model of bitter masking compounds derived or related to flavonoids is able to explain the structure–activity relationships qualitatively. To check the value of the model, the activities of enterodiol (**28**) and enterolactone (**27**) were predicted. Both structures interact with the pharmacophore sites F1, F4, and F7. The *meta*-hydroxyl group of **28** interacts with the proton acceptor site F2, whereas the *meta*-hydroxyl group of **27** interacts with the proton acceptor site F9. Enterodiol (**28**) but not enterolactone (**27**) is additionally able to interact with the proton acceptor/donor site F3 and makes contact to the hydrophobic interaction sites F6 and F8. This indicates that **28** might act

as an inhibitor for the bitter receptor, whereas **27** will enforce a conformational change of the receptor to get a better fit. To verify the prediction, enterolactone (**27**) and enterodiol (**28**) were also tested for their bitter modulating activity (Table 4).

Table 4. Evaluation of MEs for Bitter Taste of Enterolactone (**27**) and Enterodiol (**28**) against 500 mg L⁻¹ Caffeine^a

compd	bitter modulation 500 mg L ⁻¹ caffeine		
	panelists all/masking	ME for bitter taste	additional descriptors
27	14/4	29%	dull, earthy, mold, soapy
28	14/4	-31% (<i>p</i> = 0.08)	somewhat dull, earthy

^aTest concentration, 25 mg L⁻¹; ND, not determined.

Indeed, **28** (25 mg L⁻¹) showed a reasonably good masking activity against bitterness of a 500 mg L⁻¹ caffeine solution in the duo comparison, whereas the test solutions containing caffeine and enterolactone (**27**) were judged more bitter by the panelists as compared to the control. These results demonstrate the predictive power of the pharmacophore model.

■ ASSOCIATED CONTENT

Supporting Information

Syntheses and materials and methods. This material is available free of charge via the Internet at <http://pubs.acs.org>.

■ AUTHOR INFORMATION

Corresponding Author

*Tel: +49(0)5531 90 1883. Fax: +49(0)5531 90 48883. E-mail: jakob.ley@symrise.com.

Notes

The authors declare no competing financial interest.

Parts of this study were presented as a poster at the 12th Weurman Flavor Research Symposium, July 1–4, 2008, Interlaken, Switzerland.

ACKNOWLEDGMENTS

We thank the analytical department (Dr. B. Weber, M. Roloff, and Dr. A. Degenhardt) for support and Dr. H.-J. Bertram for initiation of this work.

REFERENCES

- (1) Ley, J. P. Masking Bitter Taste by Molecules. *Chemosensory Perception* **2008**, *1* (1), 58–77.
- (2) Soldo, T.; Blank, I.; Hofmann, T. (+)-(S)-Alapyridaine—A general taste enhancer? *Chem. Sens.* **2003**, *28*, 371–379.
- (3) Soldo, T.; Hofmann, T. Application of Hydrophilic Interaction Liquid Chromatography/Comparative Taste Dilution Analysis for Identification of a Bitter Inhibitor by a Combinatorial Approach Based on Maillard Reaction Chemistry. *J. Agric. Food Chem.* **2005**, *53* (23), 9165–9171.
- (4) Degenhardt, A.; Ullrich, F.; Hofmann, T.; Stark, T. Flavonoid sugar addition products, method for manufacture and use thereof as flavoring materials. EP 1,856,988.
- (5) Matuschek, M.; Jager, M. B.; Kleber, A.; Krohn, M.; Zinke, H. Method for modulating the taste of material compositions containing at least one high intensity sweetener (his). WO 2008 102,018, 2008.
- (6) Slack, J. P.; Brockhoff, A.; Batram, C.; Menzel, S.; Sonnabend, C.; Born, S.; Galindo, M. M.; Kohl, S.; Thalmann, S.; Ostopovici-Halip, L.; Simons, C. T.; Ungureanu, I.; Duineveld, K.; Bologna, C. G.; Behrens, M.; Furrer, S.; Oprea, T. I.; Meyerhof, W. Modulation of Bitter Taste Perception by a Small Molecule hTAS2R Antagonist. *Curr. Biol.* **2010**, *20* (12), 1104–1109.
- (7) Ley, J. P.; Krammer, G.; Reinders, G.; Gatfield, I. L.; Bertram, H. J. Evaluation of Bitter Masking Flavanones from Herba Santa (*Eriodictyon californicum* (H. & A.) Torr., Hydrophyllaceae). *J. Agric. Food Chem.* **2005**, *53* (15), 6061–6066.
- (8) Ley, J. P.; Blings, M.; Paetz, S.; Krammer, G. E.; Bertram, H.-J. New Bitter-Masking Compounds: Hydroxylated Benzoic Acid Amides of Aromatic Amines as Structural Analogues of Homoeriodictyol. *J. Agric. Food Chem.* **2006**, *54* (22), 8574–8579.
- (9) Ley, J. P.; Paetz, S.; Blings, M.; Hoffmann-Lücke, P.; Bertram, H.-J.; Krammer, G. E. Structural Analogues of Homoeriodictyol as Flavor Modifiers. Part III: Short Chain Gingerdione Derivatives. *J. Agric. Food Chem.* **2008**, *56* (15), 6656–6664.
- (10) MOE [2008.10]; Chemical Computing Group Inc.: Montreal, Canada, 2009.
- (11) Halgren, T. A. Merck molecular force field 0.1. Basis, form, scope, parameterization, and performance of MMFF94. *J. Comput. Chem.* **1996**, *17*, 490–519.
- (12) Halgren, T. A. Merck molecular force field 0.2. MMFF94 van der Waals and electrostatic parameters for intermolecular interactions. *J. Comput. Chem.* **1996**, *17*, 520–552.
- (13) Halgren, T. A. Merck molecular force field 0.3. Molecular geometries and vibrational frequencies for MMFF94. *J. Comput. Chem.* **1996**, *17*, 553–586.
- (14) Halgren, T. A.; Nachbar, R. B. Merck molecular force field 0.4. Conformational energies and geometries for MMFF94. *J. Comput. Chem.* **1996**, *17*, 587–615.
- (15) Halgren, T. A. Merck molecular force field 0.5. Extension of MMFF94 using experimental data, additional computational data, and empirical rules. *J. Comput. Chem.* **1996**, *17*, 616–641.
- (16) Okada, T.; Sugihara, M.; Bondar, A. N.; Elstner, M.; Entel, P.; Buss, V. The Retinal Conformation and Its Environment in Rhodopsin in Light of a New 2.2 Å Crystal Structure. *J. Mol. Biol.* **2004**, *342* (2), 571–583.
- (17) Pieper, U.; Eswar, N.; Braberg, H.; Madhusudhan, M. S.; Davis, F. P.; Stuart, A. C.; Mirkovic, N.; Rossi, A.; Marti-Renom, M. A.; Fiser, A. MODBASE, a Database of Annotated Comparative Protein Structure Models, and Associated Resources. *Nucleic Acids Res.* **2004**, *32* (Suppl. 1), D217–D222.
- (18) Laskowski, R. A.; MacArthur, M. W.; Moss, D. S.; Thornton, J. M. PROCHECK: A Program to Check the Stereochemical Quality of Protein Structures. *J. Appl. Crystallogr.* **1993**, *26* (2), 283–291.
- (19) Sippl, M. J. Recognition of Errors in Three-dimensional Structures of Proteins. *Proteins: Struct., Funct., Bioinf.* **1993**, *17* (4), 355–362.
- (20) Krieger, E.; Darden, T.; Nabuurs, S. B.; Finkelstein, A.; Vriend, G. Making Optimal Use of Empirical Energy Functions: Force-field Parameterization in Crystal Space. *Proteins: Struct., Funct., Bioinf.* **2004**, *57* (4), 678–683.
- (21) YASARA, version 11.4.18; Radboud University: Nijmegen, Netherlands, 2011.
- (22) Duan, Y.; Wu, C.; Chowdhury, S.; Lee, M. C.; Xiong, G.; Zhang, W.; Yang, R.; Cieplak, P.; Luo, R.; Lee, T. A Point-charge Force Field for Molecular Mechanics Simulations of Proteins Based on Condensed-phase Quantum Mechanical Calculations. *J. Comput. Chem.* **2003**, *24* (16), 1999–2012.
- (23) GOLD, version 4.1; The Cambridge Crystallographic Data Centre: Cambridge, United Kingdom, 2009.
- (24) Logendra, S.; Ribnicky, D. M.; Yang, H.; Poulev, A.; Ma, J.; Kennelly, E. J.; Raskin, I. Bioassay-guided isolation of aldose reductase inhibitors from *Artemisia dracunculoides*. *Phytochemistry* **2006**, *67* (14), 1539–1546.
- (25) Tanaka, T.; Yamasaki, K.; Kohda, H.; Tanaka, O.; Mahato, S. B. Dihydrochalcone-glucosides as sweet principles of *Symplocos* ssp. *Planta Med.* **1980**, No. Suppl., 81–83.
- (26) Chou, H.-C.; Chen, J.-J.; Duh, C.-Y.; Huang, T.-F.; Chen, I.-S. Cytotoxic and anti-platelet aggregation constituents from the root wood of *Melicope semecarpifolia*. *Planta Med.* **2005**, *71* (11), 1078–1081.
- (27) Fokialakis, N.; Lambrinidis, G.; Mitsiou, D. J.; Aligiannis, N.; Mitakou, S.; Skaltsounis, A. L.; Pratsinis, H.; Mikros, E.; Alexis, M. N. A new class of phytoestrogens: Evaluation of the estrogenic activity of deoxybenzoin. *Chem. Biol.* **2004**, *11* (3), 397–406.
- (28) Goto, H.; Terao, Y.; Akai, S. Synthesis of various kinds of isoflavones, isoflavanes, and biphenyl-ketones and their 1,1-diphenyl-2-picrylhydrazyl radical-scavenging activities. *Chem. Pharm. Bull.* **2009**, *57* (4), 346–360.
- (29) Ley, J. P.; Kindel, G.; Paetz, S.; Krammer, G. Hydroxydeoxybenzoin and the use thereof to mask a bitter taste. EP 1,868,452-B1, 2006.
- (30) Osaki, N.; Koyano, T.; Kowithayakorn, T.; Hayashi, M.; Komiyama, K.; Ishibashi, M. Sesquiterpenoids and Plasmin-Inhibitory Flavonoids from *Blumea balsamifera*. *J. Nat. Prod.* **2005**, *68* (3), 447–449.
- (31) Graef, C. F. F.; Vichnewski, W.; De Souza, G. E. P.; Lopes, J. L. C.; Albuquerque, S.; Cunha, W. R. A study of the trypanocidal and analgesic properties [of substances] from *Lychnophora granmangolese* (Duarte) Semir & Leitao Filho. *Phytother. Res.* **2000**, *14* (3), 203–206.
- (32) Ali, D. M.; Wong, K. C.; Lim, P. K. Flavonoids from *Blumea balsamifera*. *Fitoterapia* **2005**, *76* (1), 128–130.
- (33) Ye, J.; Guan, Y.; Zeng, S.; Liu, D. Ampelopsin prevents apoptosis induced by H₂O₂ in MT4-lymphocytes. *Planta Med.* **2008**, *74*, 252–257.
- (34) Meyerhof, W.; Batram, C.; Kuhn, C.; Brockhoff, A.; Chudoba, E.; Bufer, B.; Appendino, G.; Behrens, M. The Molecular Receptive Ranges of Human TAS2R Bitter Taste Receptors. *Chem. Senses* **2010**, *35* (2), 157–170.
- (35) Cano, J.; Mintijano, H.; Lopez-Cremades, F.; Borrego, F. Masking the bitter taste of pharmaceuticals. *Manufacturing Chemist* **2000**, No. July, 16–17.
- (36) Meyerhof, W. Elucidation of mammalian bitter taste. *Rev. Physiol., Biochem. Pharmacol.* **2005**, *154*, 37–72.
- (37) Brockhoff, A.; Behrens, M.; Roudnitzky, N.; Appendino, G.; Avonto, C.; Meyerhof, W. Receptor agonism and antagonism of dietary bitter compounds. *J. Neurosci.* **2011**, *31*, 14775–14782.